

PHOTOPRODUCTION OF JETS*

J. M. BUTTERWORTH

*Department of Physics and Astronomy, University College London, Gower St.
London, WC1E 6BT, UK
E-mail: jmb@hep.ucl.ac.uk*

On behalf of the H1 and ZEUS collaborations.

ABSTRACT

The status of HERA data on jet photoproduction is reviewed, and some suggestions and prospects for further work are given.

1. Introduction

The photoproduction of jets at HERA is proving to be a very fruitful process in which to study strong interactions. Aspects of QCD which are being investigated include the partonic structure of both the proton and the photon, the internal structure of jets, and the dynamics of jet production. I will omit jet production in association with prompt photons, charm and rapidity gaps - these reactions are covered in other contributions.

2. Starting Simply

In leading order QCD, jet photoproduction processes are divided into two classes: ‘direct’ and ‘resolved’. Example diagrams for these processes are shown in Fig.1. Direct processes are apparently simple - the photon couples directly into the hard scattering (via high virtuality quarks), and thus the fraction (x_γ) of its momentum transferred to the high E_T partons is one. However, the photon may couple to a $q\bar{q}$ pair with a relative p_T much less than the E_T of the hard jets. In this case large logarithms of E_T/p_T enter into calculations of the cross section and for the lowest p_T ’s the splitting of the photon is non-perturbative. These features lead to the introduction of a partonic structure for the photon, to describe the ‘cascade’ of partons derived from such low p_T splittings. Reactions involving partons from this cascade are called resolved photon interactions, and they enter the jet production cross section at the same order as direct processes. In this case, $x_\gamma < 1$.

An obvious first question to address at HERA then is - How well does this leading order language correspond to the actual situation in experiment? To answer it one must decide carefully what to attempt to measure. The goal should not be to somehow try to extract ‘leading order’ cross sections or variables, but to define sensible observables which have natural interpretations in the LO picture but which are well

*UCL/HEP 97-04, Presented at the Ringberg Workshop ‘New Trends in HERA Physics’, Tegernsee, Gernernay, 25-30 May 1997.

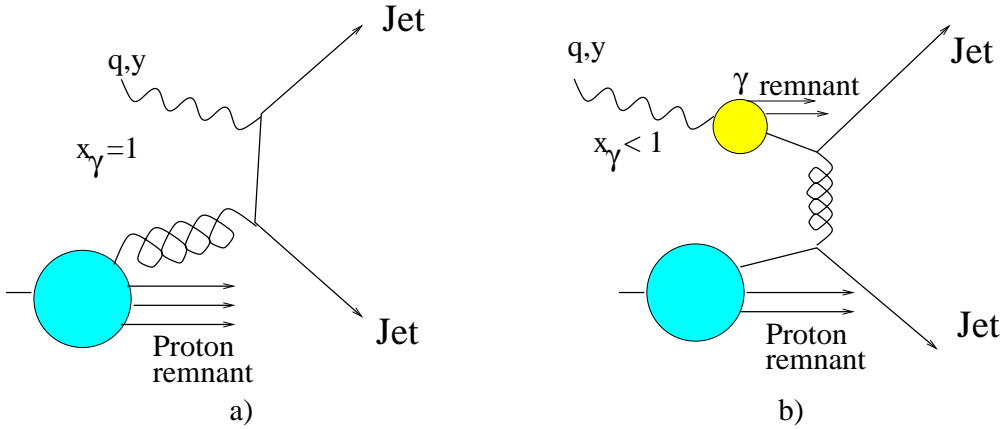


Fig. 1. Leading order diagrams for direct (a) and resolved (b) jet photoproduction.

defined independently of it.

The first such observable is a jet. At leading order this corresponds to a parton, but in experiment (as well as in more sophisticated calculations) it is defined by a jet algorithm. More of this later. For now, it is enough to remark that jets have well defined pseudorapidity^a(η^{jet}) and transverse energy (E_T^{jet}).

In photoproduction events at HERA the positron generally escapes down the beampipe. This constrains the negative of the four-momentum squared of the photon (Q^2) to be below about 4 GeV², and the median value is $Q^2 \approx 10^{-3}$ GeV². This is *not* the hard scale of the interaction (which is provided by E_T^{jet}), and is more usually referred to as P^2 in photon physics. Another important variable is the inelasticity y . This is defined in the same way as in deep inelastic scattering (DIS), but at low Q^2 it reduces to $y \approx E_\gamma/E_e$.

Using the jets and y , the variable $x_\gamma^{OBS} = \sum_{jets} (E_T^{jet} e^{-\eta^{jet}}) / 2yE_e$ is defined. It is the fraction of the photon's momentum appearing in the high E_T^{jet} jets. In dijet cross sections the sum runs over the two highest E_T^{jet} events. The superscript 'OBS' is meant to indicate that this is an observable, unlike the LO x_γ . However, in a two parton final state, x_γ^{OBS} reduces to the LO variable.

The (uncorrected) x_γ^{OBS} distribution from ZEUS¹ is shown in Fig.2. There is a clear two-component structure, with a peak at high values of x_γ^{OBS} and a rising tail to low values, which is cut off eventually by detector acceptance. Also shown are the distributions obtained from Monte Carlo (MC) simulations which include parton showers and hadronisation models as well as the LO diagrams. The direct MC events lie at high x_γ^{OBS} .

Thus the LO QCD picture has passed its first test (at least qualitatively - there are discrepancies at low x_γ^{OBS} between the data and the MC). There is a further test which can be made quite simply. The dominant LO diagrams for direct processes

^a $\eta = -\ln \tan \theta/2$ where θ is the polar angle of the jet w.r.t. the proton direction.

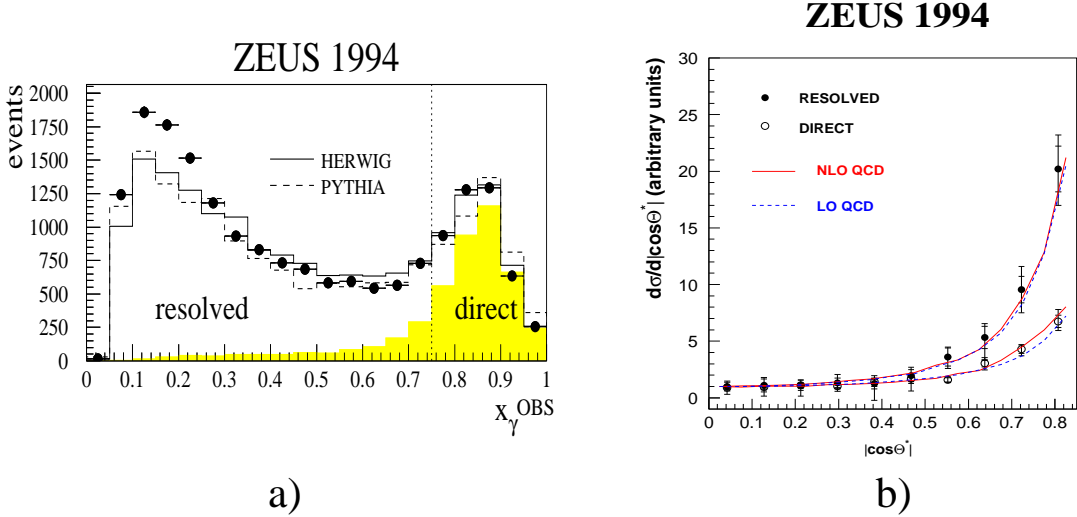


Fig. 2. a) Uncorrected x_γ^{OBS} distribution b) dijet angular distributions.

involve fermion (i.e. quark) exchange whereas those in resolved processes involve boson (i.e. gluon) exchange (see Fig.1). This leads to different predictions for the dijet angular distribution in the jet-jet centre-of-mass frame. The direct (high x_γ^{OBS}) should be distributed according to $|1 - \cos\theta^*|^{-1}$, whereas the resolved (low x_γ^{OBS}) should be $\approx |1 - \cos\theta^*|^{-2}$. ZEUS has measured these distributions² for dijet invariant mass above 23 GeV. The results are shown in Fig.2. The data agree well with the predictions. Also shown are NLO calculations from Harris and Owens³, which agree well with both the data and with the LO curves.

3. Jet Cross Sections

So far the simple LO picture of these processes is in pretty good shape. What else can we learn? As well as being sensitive to the QCD dynamics, jet cross sections are sensitive to the parton distributions in the photon and the proton. Thus in principle they can give information about the quark and gluon distributions inside the photon and proton. H1 and ZEUS have measured inclusive and dijet cross sections and the statistics are now becoming sufficiently high for measurements of multijet jet cross sections to begin.

3.1. Inclusive Jet Cross Sections

Both ZEUS and H1 measure inclusive jet cross sections differential in η^{jet} and integrated above a given E_T^{jet} , and cross sections differential in E_T^{jet} integrated within a range of η^{jet} . All the cross sections are ep cross sections integrated within specified y and Q^2 ranges.

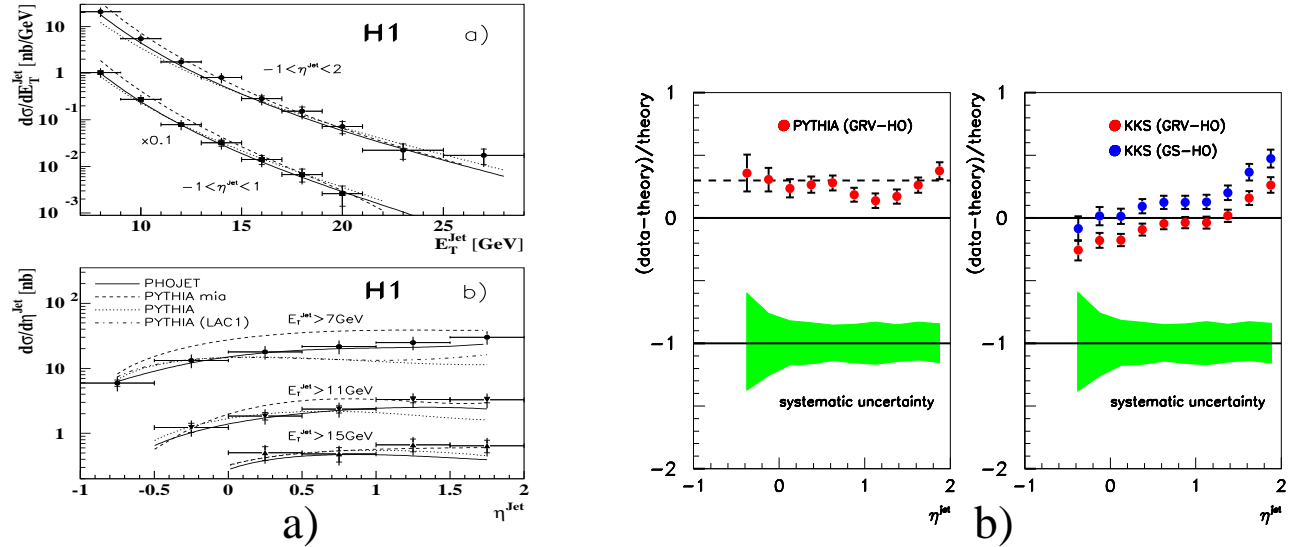


Fig. 3. Inclusive jet cross sections. The H1 data⁴ have a normalisation uncertainty of 26% which is not shown. The uncertainty in the ZEUS data arising from the energy scale of the calorimeter is correlated between points and is indicated by the shaded band. The ZEUS data show the difference between data and theory for the cross section $d\sigma/d\eta^{\text{jet}}$ for $E_T^{\text{jet}} > 17$ GeV⁶.

Some examples are shown in Fig.3. The H1 data⁴ are compared to the expectations of LO MC simulations. For the standard PYTHIA there is in general reasonable agreement in the shape at high E_T^{jet} values. However, at low E_T^{jet} and in the forward region the data lie above the MC (whether GRV or LAC1 parton distributions are used for the photon). The other MC models shown contain multiparton interactions and give higher cross sections - more of this later. An example of the ZEUS inclusive jet data is also shown. This time, the difference between data and ‘theory’ is plotted, where in the first case the theory is PYTHIA again, and in the second case it is a NLO QCD calculation from Klasen and Kramer⁵. For these higher E_T^{jet} values PYTHIA lies below the data over the whole range. The NLO QCD calculations describe the normalisation of the data better, but lie below the data in the forward region. The sensitivity to the parton distribution in the photon is similar in size to the systematic uncertainties in the measurement.

3.2. Dijet Cross Sections

Once two (or more) jets per event are measured in the detector, many possible cross sections can be measured. The angular distributions shown earlier are an example, as might be the x_γ^{OBS} distribution. A choice which has been made by ZEUS¹ is to measure $d\sigma/d\bar{\eta}$ for both jets above a given E_T^{jet} cut. Here $\bar{\eta} \equiv (\eta_1 + \eta_2)/2$ is the

boost of the dijet system in the lab frame. Rewriting $x_\gamma^{OBS} \approx E_T^{jet} e^{-\bar{\eta}} \cosh \Delta\eta / y E_e$ shows that for small $|\Delta\eta| \equiv |\eta_1 - \eta_2|$ the smallest x values are probed for a given E_T^{jet} . Scanning across $\bar{\eta}$ means scanning across yx_γ and x_p . Low $\bar{\eta}$ means high x_γ and low x_p (typically 0.005). High $\bar{\eta}$ means low x_γ and moderate x_p (typically 0.1). The cross section is measured in two x_γ^{OBS} regions corresponding to direct ($x_\gamma^{OBS} > 0.75$) and resolved ($0.3 < x_\gamma^{OBS} < 0.75$). The data are shown in Fig.4.

3.3. Comments on Jet Cross Sections

The situation now looks a little less clear. There is reasonable agreement between data and theory for dijet cross sections at high x_γ^{OBS} , but the calculations are too low at low E_T^{jet} and low x_γ^{OBS} . There is reasonable agreement in backward inclusive jets, but the calculation is too low in the forward direction, particularly for the lowest E_T^{jet} values measured. The next section contains some possible explanations and hints at how these discrepancies might be resolved.

4. What is a jet?

The theory we wish to investigate is QCD. Although MC simulations describe some event properties more successfully by use of phenomenological models, the best calculations available are at next-to-leading order in α_s and do not include effects such as hadronisation. This means that although in nature jets consist of many (typically more than five) hadrons, in the theory they consist of two (at most) partons. These partons are the hardest in the event, and thus can be expected to give a reasonable description of high E_T^{jet} jets. However, the following issues (and maybe others!) must be addressed before strong conclusions can be drawn from comparisons between data and theory. None of them are trivial issues, and the investigation of them should deepen our understanding significantly.

4.1. Jet Algorithms

It is not correct to think of jets as being simply ‘smeared’ partons. Jets are defined by an algorithm. Are the algorithms the same in experiment and theory? Experiments have used cone algorithms of various flavours or more lately a mode of the so-called k_T cluster algorithm which uses separation in $\eta - \phi$ space as its distance parameter⁷. So far the calculations have used only a cone algorithm.

A major source of ambiguity arises in the seed finding (that is, where do you begin looking for a jet?) and jet merging and/or splitting (that is, at what point does a fairly hard subjet become an extra jet in its own right?). The details of how these are performed can have a large effect on the experiment and a lesser or different one on the theory. No unique treatment is defined in the famous Snowmass convention⁸.

ZEUS 1994 preliminary

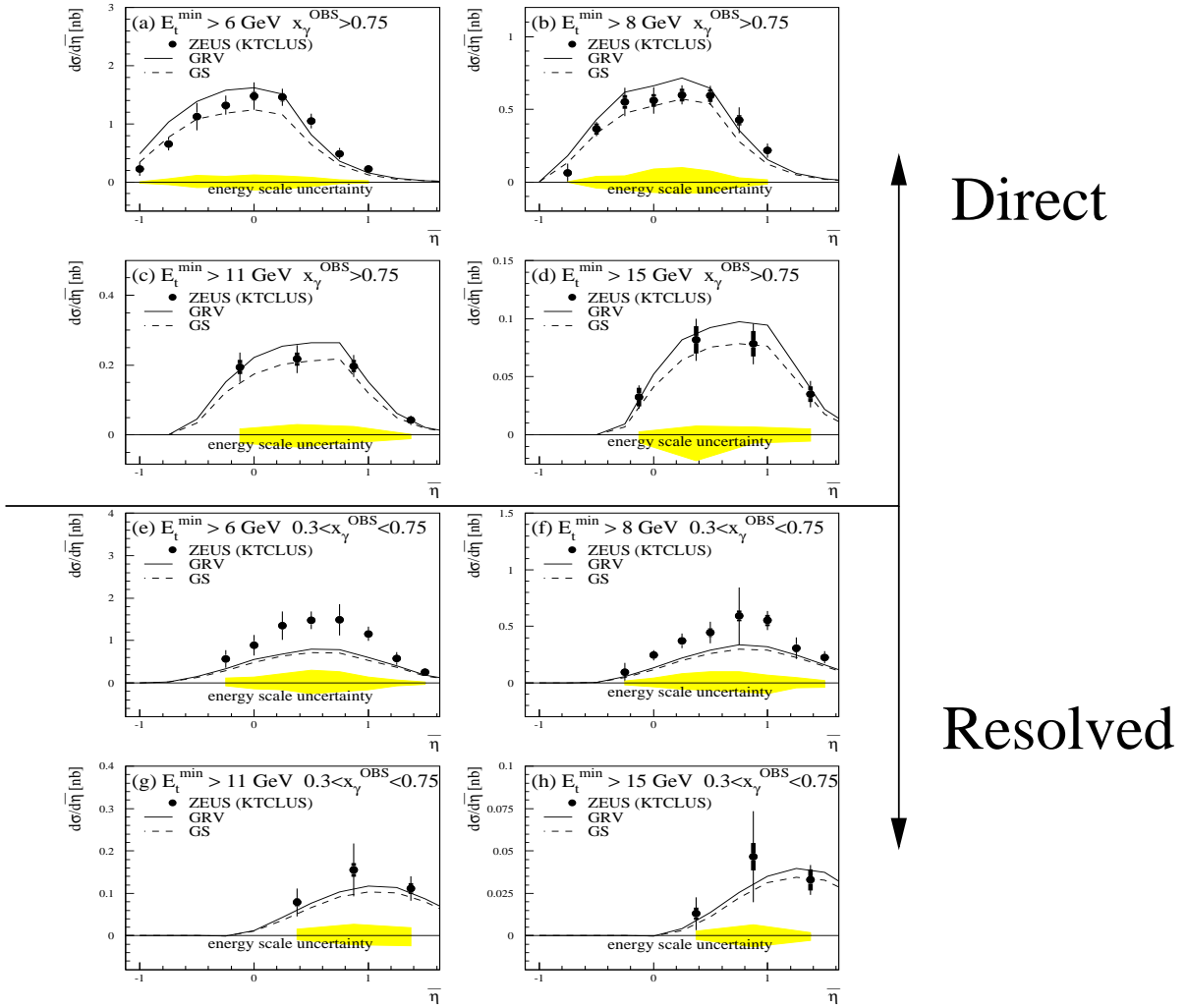


Fig. 4. Dijet cross sections from ZEUS¹. The uncertainty in the data arising from the energy scale of the calorimeter is correlated between points and is indicated by the shaded band.

A particular example of a problem can be seen by considering two partons or hard particles separated by $\delta r = \sqrt{\delta\phi^2 + \delta\eta^2} = 2$. An experimental cone algorithm running with jet radius $R = 1$ would typically take one of these (or the calorimeter cluster caused by it) and draw a circle of radius one around it. No other particle is inside this radius and so a stable jet is formed. The second particle will form a second jet. However, in a theoretical calculation the partons will be merged (if they have the same E_T) because they *do* both lie within a cone of radius one centred on their midpoint.

The parameter R_{sep} is introduced in the theory to combat this problem⁹. Partons separated by a distance greater than R_{sep} will never be merged by the algorithm. In this way, calculations attempt to mimic the effects of the seed finding stage of experimental jet finders. As a bonus, setting $R_{\text{sep}} = R$ makes the results of the cone algorithm identical (for a three parton final state) to the k_T version employed by the experiments.

Therefore one approach is to measure and calculate jet cross sections with various jet algorithms and see how changes in the algorithm affect the comparison between the two¹⁰. However, the R_{sep} method is in fact badly defined for higher order calculations, and in fact cone algorithms like this are not infrared safe in four-parton final states¹¹.

4.2. Underlying Events

Jets are not the only things in an event. How does the rest of the event affect them? The term ‘underlying event’ is often used loosely to refer to the activity in real events caused by the fact that, having provided partons for a hard scattering, the remnants of the proton and photon do not just go away. The models and language used to describe them vary widely and depending upon taste or convention effects such as initial and final state QCD radiation and soft or hard remnant-remnant interactions may or may not be included. They *do not* however include second photon-proton interactions in a single bunch crossing - the probability for this leading to significant activity in an event is negligible at HERA.

That an underlying event exists in photoproduction at HERA is clearly seen in Fig.5a. Here H1⁴ have plotted the mean transverse energy *outside the jet* per unit of $\eta - \phi$ space, as a function of x_γ^{OBS} . First, there is clearly plenty of transverse energy in the event apart from the hard jets, and secondly it is correlated to x_γ^{OBS} . Given the fact that any transverse energy outside the jet must contain some of the photon’s momentum, it is plain from the definition of x_γ^{OBS} that such a correlation must exist. However, the amount of transverse energy involved and strength of the correlation are remarkable. The implication is that this underlying event could indeed affect the jets significantly, and that it cannot be treated as independent of the jets. The size of the underlying event is correlated to the hard process, and therefore no technique relying on subtraction of typical ‘minimum bias’ events will be able to correct for it properly.

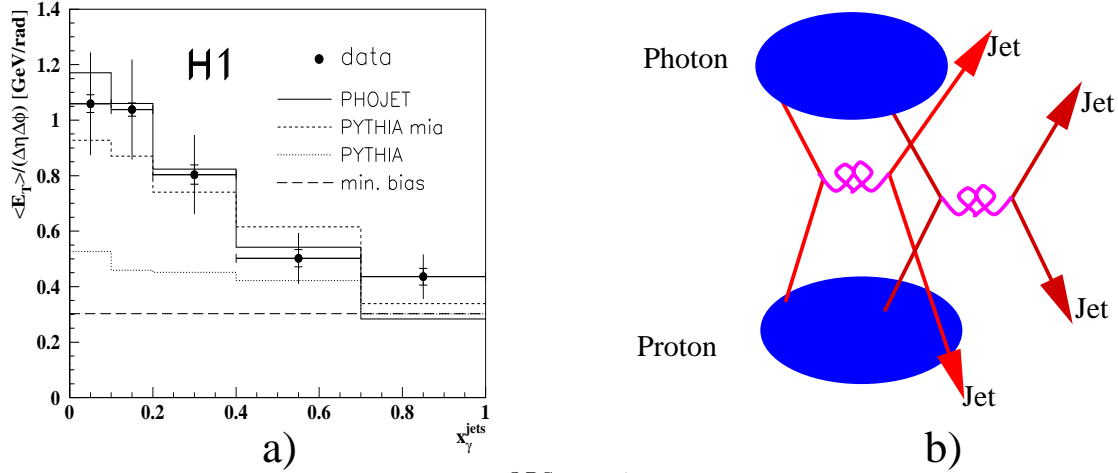


Fig. 5. (a) Energy flow outside the jets vs x_γ^{OBS} ($\equiv x_\gamma^{\text{jets}}$). (b) Schematic representation of multiparton interactions.

That such techniques have occasionally been used at hadron-hadron colliders without large ill effects seems to be because all the events are at low x , whereas the correlation becomes important in the range above $x \approx 0.1$.

A possible explanation of this type of effect is offered by multiparton interactions (MI)^{12,13}. These are allowed in eikonal models for extra hard (or sometimes soft) scatters in a single γp event, as illustrated in Fig.5b. Such models are available in PYTHIA¹⁴, HERWIG¹⁵ and PHOJET¹⁶ (but not in NLO QCD!). These models improve the description of the data - they increase energy flow around the jet core and in general increase jet cross sections. The price paid is that when MI are allowed, the energy flow outside the jet becomes very sensitive to the parton distributions in the photon and proton, and to p_T^{\min} , the cutoff for hard scattering¹³. This is because the average number of partonic interactions in a given γp event goes up with increasing parton density.

4.3. Jet Shapes

Jets have internal structure. Does the theory describe this properly? Measurements of jet shapes provide a useful way of looking at this. The jet shape $\Psi(r)$ is defined as the average fraction of the jet's transverse energy lying within cone of radius r . It is defined such that $\psi(R) = 1$. The rate at which it approaches unity as r approaches R is a measure of how collimated the jet is. ZEUS have measured jet shapes¹⁷ for a sample inclusive jets with $E_T^{\text{jet}} > 14$ GeV. An example of the data is shown in Fig.6. In Fig.6a the fraction of E_T^{jet} contained within a sub-cone of radius

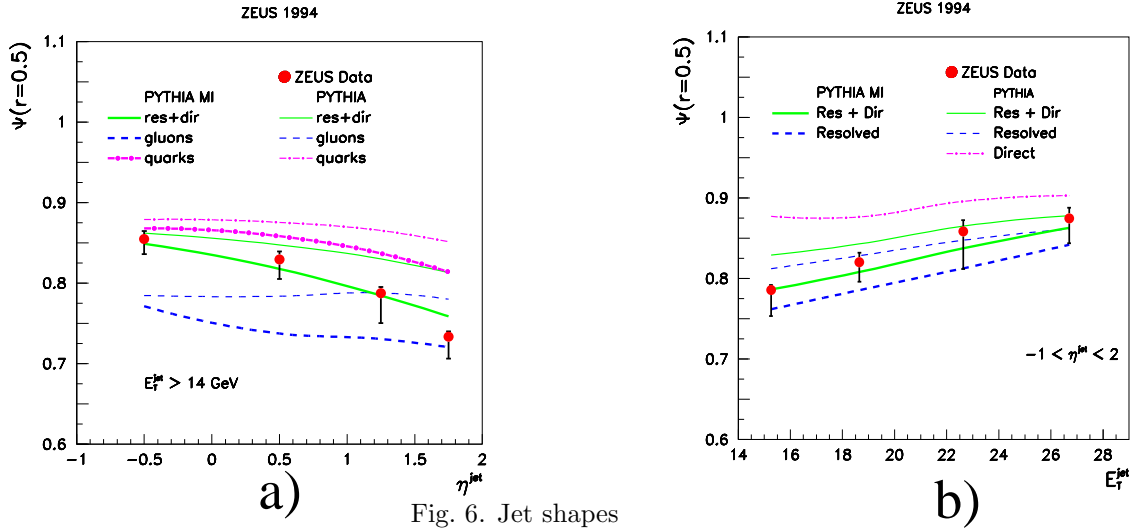


Fig. 6. Jet shapes

0.5 is plotted as a function of η^{jet} . The data show that forward jets are broader; that is, the fraction of E_T^{jet} within the inner cone decreases as η^{jet} increases. Also shown are several curves from PYTHIA. The two continuous lines show the prediction of PYTHIA with (thicker) and without (thinner) MI. Clearly, MI once more improve the description of the data. Also shown separately are the shapes for those PYTHIA jets which are initiated by a gluon or a quark at LO. Gluon jets are broader in the MC, as expected from the fact that their larger colour charge leads to more QCD radiation. The jets in the rear direction look like quark jets, whereas the behaviour is gluon like in the forward direction. The transition between the two is reproduced in the MC, where it arises from the transition from dominantly direct to dominantly resolved processes as η^{jet} increases. In Fig. 6b, the same quantity is plotted, but now as a function of E_T^{jet} . Jets get narrower as E_T^{jet} increases. In addition, in the MC the effect of multiparton interactions decreases. Comparisons to QCD calculations are given in Klasen's presentation.

5. Outlook and Conclusion

A theme in this area of physics is the benefit (and difficulty) of making general comparisons. There has been significant progress in our understanding of how to compare data and theory. The choice of jet algorithm has been discussed in this context and an attractive solution to the problems involved seems to be offered by k_T algorithm, which by virtue of being a cluster rather than cone algorithm avoids in a natural manner all seed finding and jet merging ambiguities (and hence the need for R_{sep}), but which in the chosen mode preserves the attractive features of cone

algorithms in hadronic physics.

Another point to bear in mind is that we need to choose ‘theory friendly’ cross sections. In particular, demanding two jets above a certain E_T leads to divergences in NLO QCD which are responsible for discrepancies between theoretical calculations^{3,5}. The problem is discussed in Klasen’s contribution. Recent preliminary ZEUS data¹⁸ avoid this problem by symmetrising dijet cross sections and cutting on the highest E_T^{jet} whilst applying a different and lower threshold to the second jet, also shown by Klasen.

To make comparisons at lower E_T^{jet} with confidence, a better understanding of the ‘underlying event’ is required. Multiparton interactions are a hot topic, but have many free parameters and are based upon simplifying assumptions which may not be justified. The eventual answer is surely to measure and constrain them with data. A promising approach is to study multijet events, and the current statistics are now allowing this to begin at HERA¹⁹.

Leaving aside the theory for a moment, comparisons between data from different experiments would be greatly enhanced by the adoption of a standard set of cuts and jet algorithms for a minimal subset of jet cross sections, where this is practical. The comparison of jet physics between photoproduction and DIS is another subject which is gaining momentum, both in jet shapes and cross sections.

Photoproduction at HERA and $\gamma\gamma$ collisions at e^+e^- experiments probe the photon in complementary ways. Global fits to both jet data and F_2^γ data similar to those carried out for the proton will probably place the strongest constraints on the structure of the photon in the end. However, general physics messages can be drawn from the data in other ways. A promising approach here is to study the effective parton distributions in the photon²⁰. In resolved photoproduction, the most important matrix elements have the same angular dependence and contribute to the cross section basically according to the colour factors involved. This fact allows the dijet cross section to be written in terms of single effective matrix element and an effective parton distribution:

$$\frac{d^4\sigma}{dydx_\gamma dx_p d\cos\theta^*} = \frac{1}{32\pi s_{ep}} \cdot \frac{f_{\gamma/e}}{y} \cdot \frac{f_{eff}^\gamma}{x_\gamma} \cdot \frac{f_{eff}^p}{x_p} \cdot |M_{eff}|^2$$

where $f_{eff}(x, p_T^2) = \sum q(x, p_T^2) + \bar{q}(x, p_T^2) + \frac{9}{4}g(x, p_T^2)$. H1²¹ have measured the dijet cross section shown in Fig.7a, and extracted $f_{eff}^\gamma(x, p_T^2)$ as shown in Fig.7b. There is a positive scaling violation, as seen in F_2^γ . This is characteristic of the $\gamma \rightarrow q\bar{q}$ splitting probability, and is not present in purely hadronic structure functions.

Finally, a nice instance of feedback between the two types of experiments was recently shown in OPAL data²². In 1993, ZEUS results showed that the data are better described by MC simulations if the intrinsic k_T in the photon is increased²³. This is a way of faking the effect of the fact that in the $\gamma \rightarrow q\bar{q}$ splitting the quarks can have significant relative p_T . Following this, OPAL have used a similar trick in

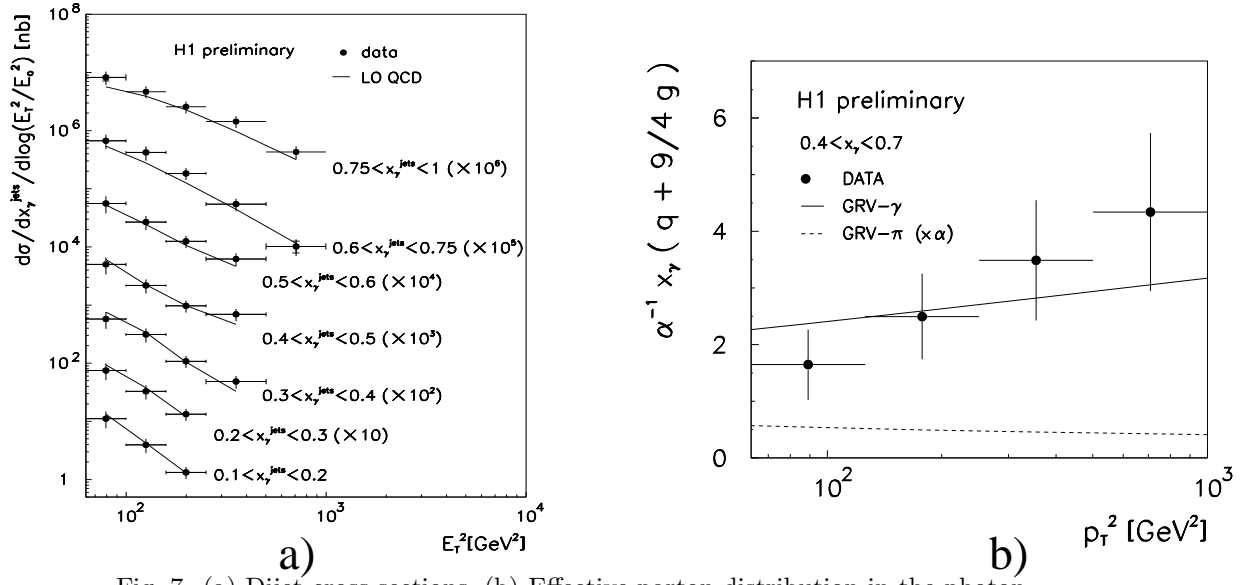


Fig. 7. (a) Dijet cross sections, (b) Effective parton distribution in the photon.

$e\gamma$ collisions to achieve a significantly better agreement in the spectrum of transverse energy outside the plane defined by the beam and the scattered electron, as well as in the dijet rates for these events.

I hope some flavour of the rapid and continuing progress in field has been conveyed. I am confident that there is a great deal more physics to come from studying jet photoproduction.

6. Acknowledgements

My thanks go to the many people on H1 and ZEUS who provided plots. I would also like to thank the DESY directorate and MPI, as well as the organisers and participants of what was an immensely stimulating and enjoyable meeting.

7. References

1. ZEUS Collab., M. Derrick et al, *Phys. Lett.* **B348** (1995) 665; Paper submitted to ICHEP96 pa02-040.
2. ZEUS Collab., M. Derrick et al, *Phys. Lett.* **B384** (1996) 401.
3. B. W. Harris and J. F. Owens, FSU-HEP-970411, hep-ph/9704324.
4. H1 Collab., S. Aid et al., *Zeit. f. Phys.* **C70** (1996) 17.
5. M. Klasen, G. Kramer DESY-96-246, hep-ph/9611450.
6. ZEUS Collab., M. Derrick et al, *Phys. Lett.* **B342** (1995) 417; Paper submitted

to ICHEP96 pa02-041.

7. S. Catani, Yu. L. Dokshitzer, M. H. Seymour and B. R. Webber, *Nucl. Phys.* **B406** (1993) 187; S. D. Ellis, D. E. Soper, *Phys. Rev.* **D48** (1993) 3160.
8. J. E. Huth et al., Proc. of the 1990 DPF Summer Study on High Energy Physics, Snowmass, Colorado, edited by E.L. Berger, World Scientific, Singapore (1992) 134.
9. S. D. Ellis, Z. Kunszt, D.E. Soper, *Phys. Rev. Lett.* **69** (1992) 3615.
10. J. M. Butterworth, L. Feld, M. Klasen and G. Kramer, *hep-ph 9608481* Proceedings of the workshop Future Physics at HERA Editors G. Ingelman, A. DeRoeck, R. Klanner, DESY 1996, p.554.
11. W. B. Kilgore, *hep-ph/9705384*, to appear in the proceedings of *XXXII Ind Rencontres de Moriond*.
12. T. Sjöstrand and M. van Zijl, *Phys. Rev.* **D36** (1987) 2019; G. A. Schuler and T. Sjöstrand, *Phys. Lett.* **B300** (1993) 169; *Nucl. Phys.* **B407** (1993) 539; J. M. Butterworth and J. R. Forshaw, *J. Phys.* **G19** (1993) 1657; R. Engel, *Z. Phys.* **C66** (1995) 203.
13. J. M. Butterworth, J. R. Forshaw and M. H. Seymour, *Zeit. f. Phys.* **C72** (1996) 637.
14. T. Sjöstrand, *Comp. Phys. Comm.* **82** (1994) 74.
15. G. Marchesini et al, *Comp. Phys. Comm.* **67** (1992) 465.
16. R. Engel, *Zeit. f. Phys.* **C66** (1995) 203.
17. ZEUS Collab., paper submitted to ICHEP96 pa02-043.
18. M. E. Hayes, for the ZEUS Collab., to appear in the proceedings of Photon '97, World Scientific.
19. E. Strickland, for the ZEUS Collab., to appear in the proceedings of Photon '97, World Scientific.
20. B. L. Combridge and C. J. Maxwell, *Nucl. Phys.* **B239** (1984) 429.
21. H1 Collab., paper submitted to ICHEP96 pa02-080.
22. J. A. Lauber, to appear in the proceedings of Photon '97, World Scientific.
23. ZEUS Collab., M. Derrick et al, *Phys. Lett.* **B354** (1995) 163.